

Quercetin induces cytochrome-c release and ROS accumulation to promote apoptosis and arrest the cell cycle in G2/M, in cervical carcinoma: signal cascade and drug-DNA interaction

K. Bishayee*, S. Ghosh*, A. Mukherjee*, R. Sadhukhan†, J. Mondal* and A. R. Khuda-Bukhsh*

*Department of Zoology, Cytogenetics and Molecular Biology Laboratory, University of Kalyani, Kalyani-741235, West Bengal, India and

†Department of Biochemistry and Biophysics, University of Kalyani, Kalyani-741235, West Bengal, India

Received 24 September 2012; revision accepted 27 November 2012

Abstract

Objectives: Small aromatic compounds like flavonoids can intercalate with DNA molecules bringing about conformational changes leading to reduced replication and transcription. Here, we have examined one dietary flavonoid, quercetin (found in many fruit and vegetables), for possible anti-cancer effects, on HeLa cells originally derived from a case of human cervical cancer.

Material and methods: By circular dichroism spectroscopy we tested whether quercetin effectively interacted with DNA to bring about conformational changes that would strongly inhibit proliferation and migration of the HeLa cells. Cytotoxic effects of quercetin on cancer/normal cells, if any, were determined by MTT assay and such depolarization of mitochondrial membrane potential, as a consequence of quercetin treatment, and accumulation of reactive oxygen species (ROS) also were studied, by FACS analysis and expression profiles of different anti- and pro-apoptotic genes and their products were determined.

Results: Quercetin intercalated with calf thymus cell DNA and HeLa cell DNA and inhibition of anti-apoptotic AKT and Bcl-2 expression were observed. Levels of mitochondrial cytochrome-c were elevated and depolarization of mitochondrial membrane potential occurred with increase of ROS; upregulation of expression of p53 and caspase-3 activity were also noted. These alterations in

signalling proteins and externalization of phosphatidyl serine residues were involved with initiation of apoptosis. Reduced AKT expression suggested reduction in cell proliferation and metastasis potential, with arrest of the cell cycle at G2/M.

Conclusion: Quercetin would have potential for use in cervical cancer chemotherapy.

Introduction

Flavonoids compose a large class of low-molecular weight natural products, of plant origin, found ubiquitously in foodstuffs, including tea, capers, lovage, apple, onion, grapes, citrus fruits, tomato, and in all green vegetables (1) (Fig. 1a). Quercetin (also known as flavin meletin), present in various food plants, has been known to provide dietary antioxidants which exert significant anti-tumour, anti-allergic and anti-inflammatory effects (2). Of the tumours, quercetin has been reported to have a potent anti-cancer role in cases of colon, breast and lung cancers, and to play an anti-metastatic role in prostate cancer (3,4). To our knowledge, no precise study has been undertaken to delineate molecular mechanisms underlying depolarization of mitochondrial membrane potential, with ROS accumulation in mitochondria, in cells of cervical carcinoma. Earlier work carried out has reported: (i) general anti-cancer effects of quercetin (5,6); and (ii) quercetin-induced cell cycle arrest and mitochondria-mediated apoptosis, in HeLa cells (7). Thus, the present investigation was undertaken with a view to understanding molecular mechanisms of quercetin's action, which have not been studied earlier.

Chemotherapy to treat cancer was introduced more than 50 years ago, and has generally shown considerable efficiency for the treatment of testicular cancer and certain leukaemias, but in general its success rate against breast, colon, lung and cervical cancers has been less

Correspondence: A. R. Khuda-Bukhsh, Department of Zoology, University of Kalyani, Kalyani-741235, West Bengal, India. Tel.: +91 33 25828750 (Extn. 315); Fax: +91 33 25828282; E-mail: prof_arkb@yahoo.co.in; khudabukhsh_48@rediffmail.com

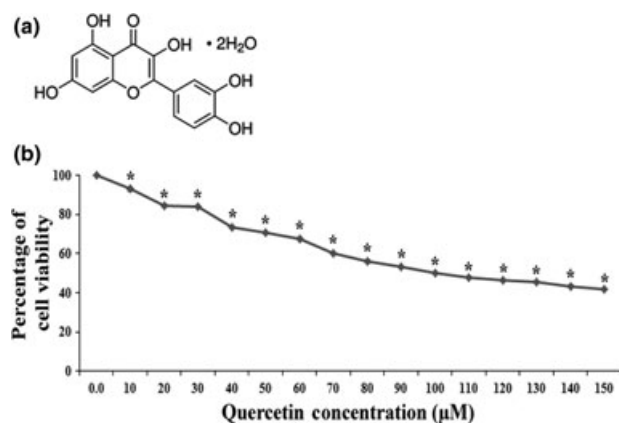


Figure 1. (a) Quercetin structure. (b) Percentage of cell viability: 10–150 μM quercetin were supplemented in culture; cell viability was determined by MTT assay and plot shows gradual reduction in viability of HeLa cells. 50% cell viability was achieved at $110.38 \pm 0.66 \mu\text{M}$ of quercetin at 18 h.

than spectacular. Ideally, chemotherapeutic drugs should specifically target neoplastic cells only and should reduce tumour burden by inducing cytotoxic and/or cytostatic effects, with minimal collateral damage to neighbouring normal cells (8).

It has now been proven that capacity of a drug to interact with DNA is reflected as a significant feature in the field of new anti-cancer therapeutic design. DNA intercalation and groove binding by exogenous molecules have attracted considerable interest in medicinal chemistry, as such complex formations lead to significant modification in DNA structure, and may result in hindered or suppressed function of nucleic acids in physiological processes (9). As such influence on biological systems is a main requirement for DNA-targeting drugs, intercalation of small molecules into DNA may be applied in therapeutic approaches to arrest cell proliferation and destroy tumour cells, or in the case of infected tissues, by preventing/inhibiting synthesis of DNA and gene transcription (10).

Apoptosis is a complex process involving a range of genes and a variety of cytological factors. Caspase cleavage generally initiates apoptosis followed by initiation of DNA fragmentation. Activation of caspases is starts after suppression or activation of specific apoptogenic signal proteins such as those of the Bcl-2 family and/or cytochrome-c, which are further stimulated by appropriate physiological strata of cell systems such as ROS accumulation, and mitochondrial membrane depolarization (11). Previous workers have demonstrated that quercetin can inhibit population growth of HeLa cells and can induce apoptosis (5–7), but have not focussed on time-dependent changes occurring in a sequential manner that finally lead cells to apoptosis.

With such background, hypotheses to be tested in this investigation were whether: (i) quercetin acts as a DNA intercalating/groove-binding agent, producing conformational changes in the calf thymus cell DNA (CT DNA) and DNA of drug-treated HeLa cells; (ii) quercetin can trigger release of cytochrome-c from mitochondria, by disrupting membrane potential, as a consequence of ROS accumulation in HeLa cells, thereby inducing apoptosis.

Materials and methods

Cell culture

Cervical cells of the HeLa line were collected from NCCS, Pune, India and were cultured at 37 °C in DMEM (HiMedia, Mumbai, India) containing 10% heat-inactivated FBS of South American origin (Invitrogen, CA, USA) and 1% antibiotic (PSN) (HiMedia), in a humidified incubator with ambient O_2 level and 5% CO_2 (ESCO, Singapore). Cells were harvested with 0.025% trypsin-EDTA (Invitrogen) in phosphate buffered saline, were plated in required cell numbers and allowed to adhere, for the required time (hours) before treatment.

Cell viability assay

HeLa cells were dispensed into 96-well flat bottom microtitre plates (Tarson, Kolkata, India) 1×10^2 cells per well, and treated with the indicated concentrations of quercetin. After incubation with the drug, thiazolyl blue tetrazolium bromide (MTT) was added to the wells at a concentration of 10 $\mu\text{g/ml}$; plates were then incubated for 3 h at 37 °C in the dark. After incubation, colour was developed using acidic isopropanol and quercetin dose was determined at which cells' viability reduced to 50% in 18 h (12); OD was noted at 595 nm, in a microtitre plate reader (Thermo, Florida, USA).

Drug–DNA interaction

For assessment of quercetin and nuclear DNA interaction, two modes of study were performed; first interaction was checked on naked calf thymus cell DNA (CT DNA) with drug concentration of 90 μM using untreated CT DNA as control; secondly, to measure interaction of drug with DNA within cells, incubation was performed with quercetin at concentrations of 90 μM for 3 h. After 3 h incubation, cells were collected and their DNA was extracted and purified using GeneiPure Mammalian Genomic DNA Purification Kit, Bangalore, India. DNA collected was used to analyse CD spectra for determination (13) (JASCO J720,

Tokyo, Japan) and was analysed using Origin 8 Pro software (OriginLab Corporation, Northampton, MA, UK).

Cell morphological analysis

HeLa cells were plated at 1×10^3 cells per 25 mm plate (Tarson) and treated with 30, 60 and 90 μM of quercetin to determine microscopically changes in cell morphology compared to controls. After 18 h incubation, cells were observed using an inverted phase-contrast microscope (Leica, Wetzlar, Germany). They were then stained using DAPI (Sigma, Saint Louis, MO, USA) for nuclei, and AO-EB [Acridine orange-ethidium bromide] (SRL, Mumbai, India) dual stain, at 10 μM concentration each, after 4% paraformaldehyde fixation. Cells were then analysed using a fluorescence microscope (Leica).

Assessment of cell proliferation, migration and the cell cycle

To perform a cell proliferation assay, cells were incubated with 60 μM quercetin and were harvested after 0, 6, 12 and 18 h incubation, washed twice in PBS and trypsinized. Cell suspensions were then transferred for cell counting. This procedure was repeated for all samples at each time point, and experiments were repeated 3 times. After analysis of data, cell proliferation results were plotted.

To perform the migration assay, cells were seeded at 2×10^5 density per well in sterile 6-well plates. Confluent cell monolayers were scraped to create a scratch in each, with a pipette tip; first images of scratches were acquired. After quercetin treatment and incubation, plates were placed under a phase-contrast microscope, dish reference points matched, and regions of first image photographs were aligned; then second images were acquired (14).

Cells were plated at 1×10^3 cells per 25 mm plate and treated with 30, 60 and 90 μM of quercetin; after incubation for 18 h against a control set, cell cycles were analysed using PI (Sigma) (5 μl) stained cells after fixation in 70% chilled ethanol and RNase (Novagen, San Diego, CA, USA) treatment (15). PI fluorescence intensity was determined by flow cytometry using an FL-2A filter (BD FACS Calibur, San Jose, CA, USA).

Intracellular ROS accumulation

ROS accumulation was evaluated by deploying cells to both fluorescence microscopy and flow-cytometric methods. After incubation for 0, 6, 12 and 18 h in 60 μM quercetin, cells were fixed and incubated in 10 μM DCHFDA (Sigma), for 20 min in the dark. Cells were then analysed using fluorescence microscopy.

For quantitative estimation, treated cells were fixed in 70% ethanol and incubated in 10 μM DCHFDA for 30 min in cold and dark conditions, and dye fluorescence intensity was determined by flow cytometry using an FL-1H filter (15). Data were analysed using Cyflogic software (Cyflogic Team, Turku, Finland).

Changes in mitochondrial membrane potential ($\Delta\Psi\text{m}$)

Changes in mitochondrial membrane potential (MMP) were evaluated by deploying both fluorescence microscopy and flow cytometry. After incubation for 0, 6, 12 and 18 h with 60 μM of quercetin, cells were fixed and incubated in 10 μM rhodamine 123 (Sigma) for 30 min in the dark. They were then analysed using fluorescence microscopy.

For quantitative estimation of MMP, treated cells were fixed in 70% ethanol and incubated in 10 μM rhodamine 123 for 30 min in the cold and dark and dye fluorescence intensity was determined by flow cytometry with an FL-1H filter (16) (BD FACS Calibur). Data were analysed using Cyflogic software.

Analysis of apoptosis

To determine apoptosis, DNA fragmentation and annexinV-FITC/PI assays were performed.

For the DNA fragmentation assay, after treatment, cells were washed twice in phosphate-buffered saline (PBS) and incubated with DNA lysis buffer (10 mM Tris, 400 mM NaCl, 1 mM EDTA, 1% Triton X-100, RNase (0.2 mg/ml) and proteinase K (0.1 mg/ml)) overnight, then centrifuged at 1200 g at 4 $^{\circ}\text{C}$. Supernatants were then mixed with phenol-chloroform-isoamyle mixture (25:24:1) and bi-layered mixture was centrifuged at 1500 g , 4 $^{\circ}\text{C}$ for 15 min. DNA was then precipitated using 100% ethanol, from the aqueous layer and dissolved in 20 μl of Tris-EDTA buffer (10 mM Tris-HCl (pH 8.0) and 1 mM EDTA). Extracted DNA was further purified using proteinase K (SRL) and RNase A, to subtract excess proteins and RNAs, respectively. Purified DNA was separated using 1.5% agarose gel electrophoresis and bands were visualized under a UV trans-illuminator, followed by digital photography.

To determine the early and late apoptosis, control and treated HeLa cells were prepared by the method described by Chakraborty *et al.* (17), and 10 μM AnnexinV-FITC (Santa Cruz Biotechnology Inc., CA, USA) and 5 μM of PI solutions were added into each cell suspension and incubated further for 15 min at room temperature in the dark. The fluorescence was determined by flowcytometer using FL-1H and FL-2H

filters, respectively. Data were analysed using Cyflog software.

mRNA expression using the semi-quantitative reverse transcriptase-polymerase chain reaction

Messenger RNA for AKT, p53, cytochrome-c, Bax, Bcl-2, and caspase-3 were determined using the reverse transcriptase-polymerase chain reaction (RT-PCR). 5 µg total RNA from HeLa cells was DNase treated and reverse transcribed into cDNA (HiMedia and Chromous Biotech, Bangalore, India) 1 µl of which and 100 ng oligonucleotide primers (Eurofins, Bangalore, India) were used for PCR (Table 1). Hot-start PCR reactions were performed for 35 cycles and products were fractionated on 1% agarose gel stained with 5 mM ethidium bromide (18). *G3PDH* served as housekeeping gene (Table 1).

Immunoblotting

50 mg cell lysate was used for SDS-PAGE (12.5%) electrophoresis to estimate AKT, p53, Bax, Bcl-2, caspase-3 (Santa Cruz Biotechnology Inc.), then transferred to poly-vinyl-di-fluoride (PVDF) membranes. After blocking with 3% BSA, membranes were incubated with specific primary antibodies overnight, at 4 °C. Membranes were further incubated for 2 h with ALP conjugated secondary antibody (16). BCIP-NBT was used as developer and band intensities were analysed densitometrically using image J software (National Institute of Health, MD, USA).

Cytochrome-c activity assay

Equal numbers of cells were seeded in microtitre plates and retained there for 24 h for adherence. Surrounding

Table 1. Primers used in the experimental sets of semi-quantitative reverse transcriptase polymerase chain reactions

Primer name	Primer sequences
P53	Fwd 5'-GGAAATTTGTATCCCGAGTATCTG-3' Rev 5'-GTCTTCCAGTGTGATGATGGTAA-3'
AKT	Fwd 5'-CCTGGACTACCTGCACTCTCGAA-3' Rev 5'-TTGCTTTCAGGGCTGCTCAAGAAGG-3'
Cytochrome c	Fwd: 5'-ACGTGTCGACCTAATATGGGTGATGT TGAAAAGG-3' Rev: 5'-ACAGATCTTTCTCATTAGTAGCCTTTT AAG-3'
Bax	Fwd 5'-AGTAACATGGAGTGCAGAGG-3' Rev 5'-ATGGTCTGATCAGTCCGG-3'
Bcl-2	Fwd 5'-GTGACTTCCGATCAGGAAGG-3' Rev 5'-CTTCCAGACATTCCGAGACC-3'
Caspase 3	Fwd: 5'-AGGGTTCATTATGGGACA-3' Rev: 5'-TACACGGGATCTGTTTCTTTG-3'

media were then replaced by media devoid of FBS and cells were incubated for 0, 6, 12 and 18 h with 30, 60 and 90 µM of quercetin. Cells were then made permeable using PBS containing 0.05% Triton-x 100 and were coated with anti-cytochrome-c primary antibody, then blocked with 3% BSA in TBST. After secondary antibody incubation, PNPP was used as colour developer and colour intensity was measured at 405 nm with respect to blank.

Caspase 3 activity assay

Caspase-3 activity assay was performed using an indirect immunostaining protocol after cell incubation for 18 h in concentrations of 30, 60 and 90 µM quercetin and a control set. 5×10^6 cells were re-suspended in ice cold phosphate buffered saline with 10% FBS and 1% sodium azide. 10 µg/ml anti-caspase-3 primary antibody was added, then cells were incubated at room temperature for 30 min. After this, cells were further incubated in FITC-tagged secondary antibody for 20 min in the dark. Fluorescence was determined by flow cytometry using FL-IH filters. Data were analysed with Cyflog software.

Statistical analysis

Statistical analysis was performed by one-way ANOVA with LSD post-hoc tests, using SPSS.14 software (IBM Corporation, Armonk, NY, USA) to identify whether differences were significant among mean values of the different groups. Results are expressed as Mean ± SE (Standard Error). $P < 0.05$ was considered to be statistically significant.

Results

Quercetin treatment reduced viability of HeLa cells

Results of MTT assay revealed cell viability gradually reduced between minimal quercetin concentration to higher ones. Percentage of viability of cells at 10 µM ranged from 92.94 ± 1.06 to 41.96 ± 0.07 at 150 µM. 50% cell death occurred at 110.38 ± 0.66 µM of quercetin employment (Fig. 1).

Quercetin-induced circular dichroism spectral changes in both CT DNA and cell DNA

Circular dichroism (CD) changes are useful for determination of mobility and orientation of intercalated compounds in double-stranded DNA. Here, CD spectroscopic results revealed that quercetin disturbed

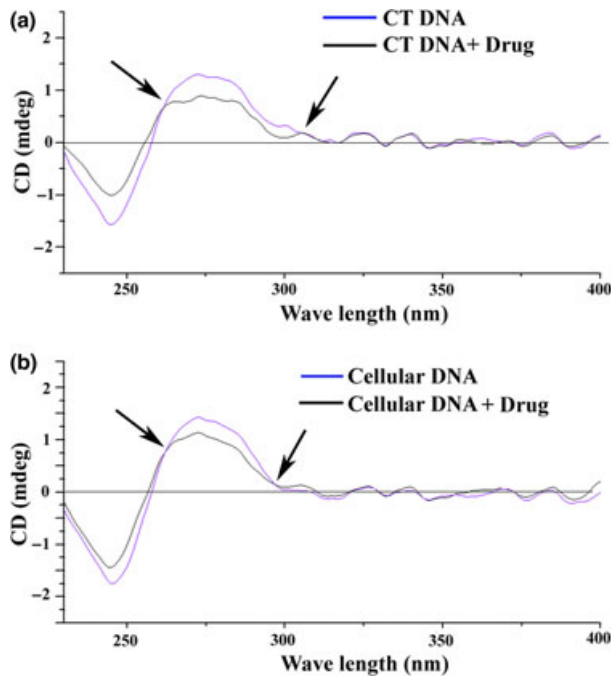


Figure 2. CD Spectral analysis: quercetin DNA binding capacity as determined by CD spectroscopy. Non-complexed calf thymus DNA and nuclear DNA displayed positive signalling at 320 and 310 nm, respectively, and no signal at 260 nm for both CT DNA (a) and nuclear DNA (b) On addition of quercetin (90 μM), the negative band decreased gradually, whereas positive signals showed hypochromism with a peak shift of 10 nm.

native B-conformation of DNA of both CT DNA and nuclear DNA of quercetin-treated HeLa cells. Non-complexed calf thymus cell DNA and nuclear DNA had positive signals at 320 and 310 nm, respectively, and no signal at 260 nm in both cases, typical features of B-DNA. On addition of quercetin to a solution of DNA, changes in its CD spectrum were observed. Negative bands decreased gradually, whereas positive signals had hypochromism with peak shift of 10 nm (Fig. 2). Such changes are likely to result from structural alterations induced by quercetin to DNA's double-helical structure. Most spectral differences are due to local structural variations along the double helix. Structural factors linked to helix, strand and sugar pucker may vary at each dinucleotide step in influencing inter-nucleotide distances and hence, base stacking.

Quercetin treatment induced morphological changes in HeLa cells, with nucleosomal fragmentation

Morphological changes were observed in HeLa cells on treatment with quercetin, with rounding of the cytoplasmic periphery along with gradual detachment of cells from substrate. Features included cell membrane blebbing and cell shrinkage in quercetin-treated cells (Fig. 3a); nucleosomal fragmentation was observed after DAPI staining, fragmentation being greatest in 90 μM

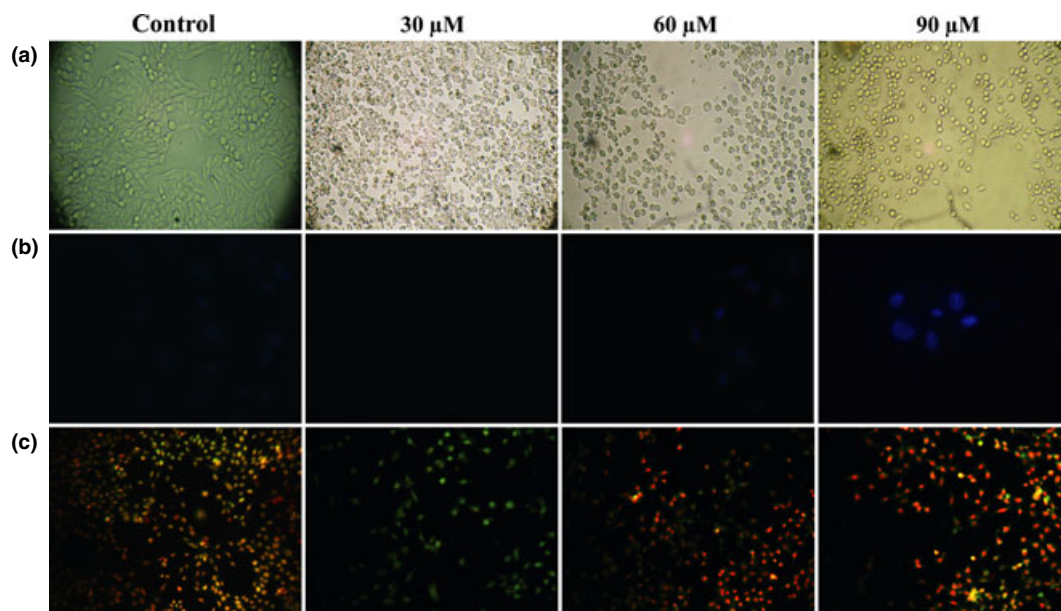


Figure 3. Microscope studies: The HeLa cells were treated with 30, 60 and 90 μM quercetin and incubated for 18 h. (a) Morphological analysis: after incubation, morphological changes were observed including cell membrane blebbing and cell shrinkage, in treated cells. (b) DAPI staining: nucleosomal fragmentation was elevated at higher quercetin doses, indicated by brighter fluorescence intensity. (c) AO/EB staining: increased numbers of apoptotic cells were determined by this staining procedure. Nuclear condensation and change in colour from green to reddish orange, of fragmented nuclear membranes, represents induction of apoptosis of treated cells compared to controls.

quercetin dose (Fig. 3b). Fluorescence intensity was observed AO/EB stained treated cells, with respect to controls (Fig. 3c). Nuclear condensation and colour change from green to reddish orange of fragmented nuclear membranes represented induction of apoptosis of treated cells compared to controls.

Quercetin treatment reduced cell proliferation and metastasis and caused cell cycle arrest

Treatment with 90 μM quercetin reduced proliferative capacity of the HeLa cells. Results of the 6-h interval study performed for 18 h showed 16% reduction in cell population growth at 6 h and 33% and 48% reduction in proliferation by 12 and 18 h, compared to controls (Fig. 4a).

The migration assay was performed to check anti-metastatic property of quercetin. It was performed for doses of 30, 60 and 90 μM for 18 h. Reduction in migration measured was 14.9%, 15.6% and 19.05% for respective doses, compared to controls (Fig. 4b).

Reduction in cell proliferation reflects cell cycle arrest at specific stages. To identify this, cell cycle analysis was performed with on 30, 60 and 90 μM quercetin on the cells. Results revealed cell density increments at G2/M phase of the cell cycle, reflecting cell cycle arrest at this stage (Fig. 4c).

Quercetin treatment gradually depolarized mitochondrial membrane potentials

Depolarization of mitochondrial membrane potential can be measured both qualitatively and quantitatively using rhodamine 123, both microscopically and flow cytometrically. Fluorescence intensity gradually reduced on quercetin treatment, compared to controls (Fig. 5a). For quantitative estimation of depolarization, FACS analysis was performed; percentage of visibility shown in Fig. 5a.

Quercetin treatment initiated ROS accumulation

Accumulation of ROS was measured by DCHFDA staining. In Fig. 5b, control cells fluoresced in green,

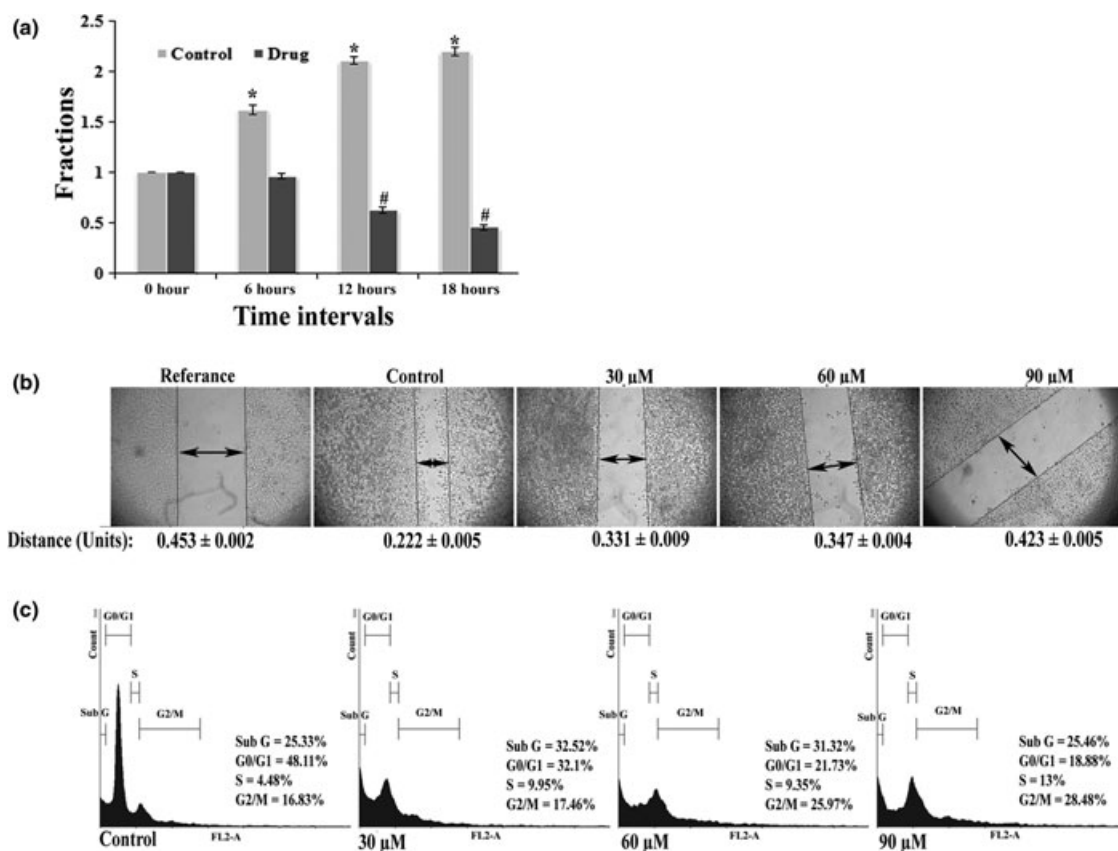


Figure 4. (a) Proliferation assay: cells were treated with 90 μM of quercetin. Reduction in proliferation was observed in treated cells. (b) Migration assay: Reduced migration was observed after quercetin treatment and reduction was measured to be 14.9%, 15.6% and 19.05% for 30, 60 and 90 μM quercetin, respectively. (c) Cell cycle analysis: cell population growth was blocked at G2/M.

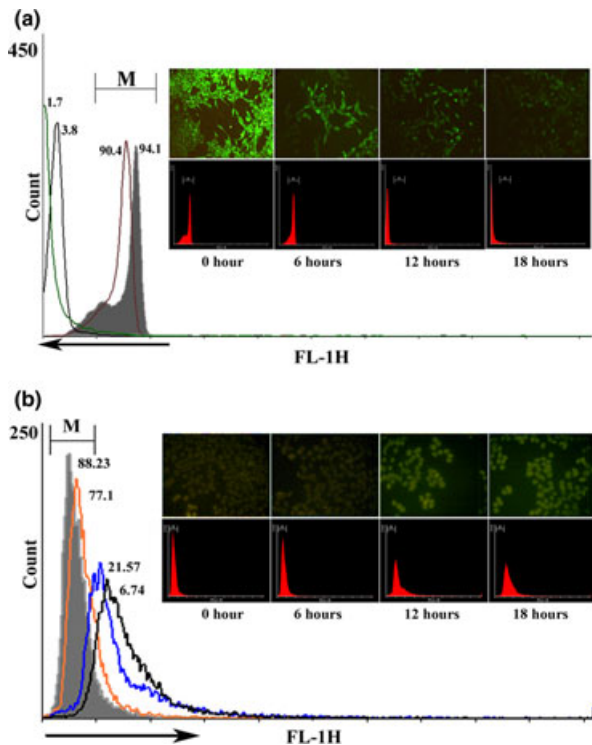


Figure 5. (a) Mitochondrial membrane potential: fluorescence intensity reduced gradually with quercetin treatment, indicating gradual depolarization of MMP. FACS studies revealed shift of peaks was towards the y-axis and was most by the 18 h. (b) ROS accumulation study: DCHFDA staining showed gradual increase in fluorescence intensity along with time, reflecting ROS accumulation. FACS data revealed peak shifted away from the y-axis with time, supporting results of microscope analysis.

while cells treated with quercetin gradually increased in fluorescence intensity along with increasing time, reflecting ROS accumulation. Quantitative data obtained by flow cytometry (Fig. 5c) also supported previous observations convincingly where it increased subsequent to increased period of quercetin exposure.

Quercetin induced plasma-membrane externalization of phosphatidyl serine with initiation of DNA fragmentation

Quantitative estimation of annexin V binding on cell surfaces was performed by FACS analysis. Whether HeLa cells externalize phosphatidyl serine when treated with quercetin was determined. Cells showed distinct positive binding with annexin V when treated with quercetin, indicating externalization of phosphatidyl serine to cell surfaces (Fig. 6a–d).

DNA fragmentation analysis results also suggested initiation of cell DNA fragmentation in quercetin-treated groups (Fig. 6e).

Effect of quercetin on gene expression related to cell death

Quercetin administration up-regulated expression of p53, BAX, cytochrome-c and caspase-3. However, expression of AKT and Bcl-2 were significantly down-regulated. *G3PDH* had served as housekeeping gene in this test (Fig. 7a).

Quercetin administration modulated different expression of protein related to cell proliferation and apoptosis

AKT expression in the HeLa cells reduced 0.9, 0.86 and 0.76-fold by the administration of quercetin at concentrations of 30, 60 and 90 μM , respectively. With AKT expression, anti-apoptotic protein Bcl-2 also was down-regulated by quercetin administration by 0.9, 0.86 and 0.86-fold, by same concentrations of drug dose. Expression of p53 and BAX was increased with quercetin administration; p53 expression was enhanced by 1.29, 1.45 and 1.57 for doses of 30, 60 and 90 μM , respectively. In the case of BAX, expression enhanced by 1.20, 1.32 and 1.49 with a similar quercetin doses (Fig. 7b).

Time-dependent study of cytochrome-c expression revealed that significant changes in its expression were seen at the 12th h of study, and by the 18th h, its expression was not significantly higher compared to the with 12-h interval value (Fig. 7c).

To check active caspase-3 percentage values after quercetin administration, caspase-3 activity assay was performed; results indicated that active caspase-3 presence was elevated from 10.67% for controls to 23.82%, 65.81% and 80.04% for quercetin dose of 30, 60 and 90 μM , respectively (Fig. 7d).

Discussion

Standard chemotherapy can be unsuccessful in treatment of cervical cancer and surgical procedures remain inadequate after initiation of metastasis (19). Moreover, unwanted side effects and/or toxicity of orthodox drugs to normal tissues and cells often render the problem complicated (8). To overcome this, DNA-targeted therapy produces better results compared to others. DNA, being a bio-receptor for vast numbers of small molecules, remains a major biological target for design of anti-cancer agents (20). Here, CD spectroscopy data revealed intercalating capacity of quercetin with CT DNA and drug-treated cell DNA. Thus, quercetin cytotoxicity could be explained by assuming that it inhibited normal processes of DNA synthesis, at some level. Static blocking capacity of quercetin is a candidate for

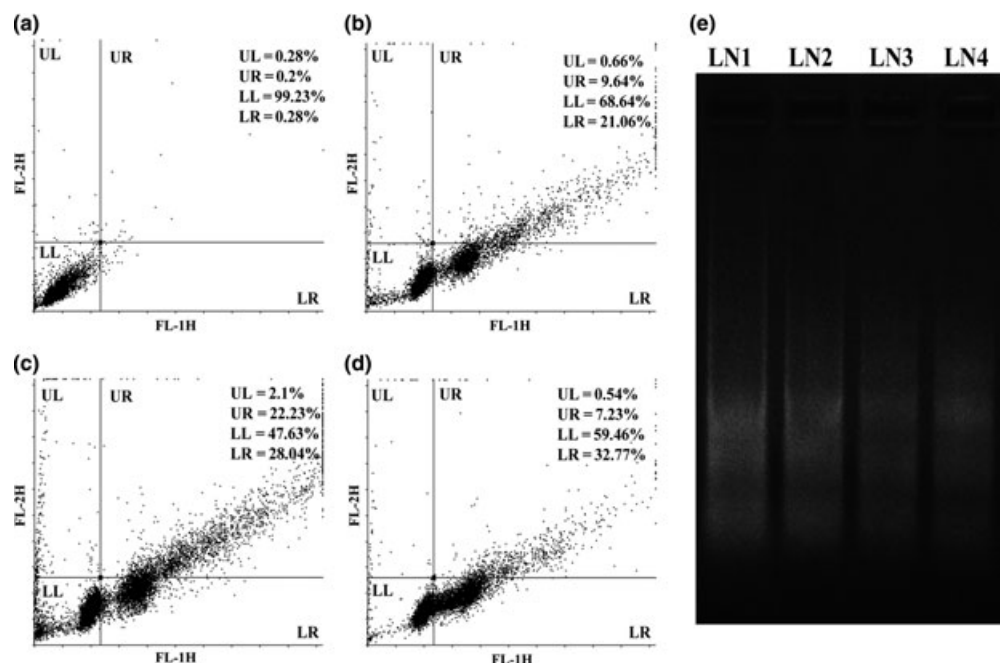


Figure 6. Assessment of externalize phosphatidyl serine by annexin V/PI assay (a–d) and DNA fragmentation assay (e): Cells were treated with 30, 60 and 90 μM quercetin and incubated for 18 h. By FACS analysis, LL- lower left, UL- upper left, LR- lower right, UR- upper right represent specific quadrants and for the DNA fragmentation study, Ln1- controls, Ln2, Ln3, Ln4- cells treated with quercetin concentrations of 30, 60 and 90 μM , respectively.

having produced apoptosis in the HeLa cells. In the present study, it was clearly shown that quercetin had the capacity to enter cells and could effectively bring about conformational changes in both calf thymus cell and HeLa cell DNA. Thus, it can logically be speculated that conformational changes in DNA played a leading role in suppressing transcription and translation for protein synthesis subsequently of HeLa cells; this in turn could initiate cell reaction cascades propelling them towards apoptosis.

The present findings also suggest that quercetin triggered cytochrome-c discharge from mitochondria which might be accelerated by accumulation of ROS in the cells; this also could be the cause of their reduced level of proliferation. These events could lead to manifestation of morphological changes in detaching cells showing condensed and fragmented chromatin. Results of MTT assay also showed that viability of the cancer cells gradually reduced with increase in dose of quercetin, a condition that was not observed in PBMCs. Analysis of apoptosis was further confirmed by data from DAPI, AO/EB staining, DNA fragmentation and annexinV/PI assay. In our findings, increase in population of cells undergoing an early-apoptotic state (manifested by cells with bright orange chromatin and highly condensed and fragmented cell boundaries) with fragmented cell DNA

was noted in the different quercetin-treated series. Thus, there was clear evidence that the drug could bring about cell events promoting apoptosis within 18 h of treatment. Results of flow cytometry were also consistent with formation of hypo-diploid cells distinguishable from debris. These qualitative and quantitative data prompt one to suggest that quercetin was able to induce apoptosis of HeLa cells within 18 h of treatment, and these had reduced migration and blocking of the cell cycle at G2/M.

Accumulation of ROS and gradient depolarization of mitochondrial membrane potential ($\Delta\Psi\text{m}$) are concurrent processes, which normally induce mitochondria to discharge cytochrome-c into the cytoplasm with rapid reduction of ATP level. Increments in cytosolic cytochrome-c enhance activity of pro-apoptotic caspase-3 for initiation of type 1 programmed cell death (21). In our findings, incremental depolarization of $\Delta\Psi\text{m}$ occurred with gradual incremental ROS accumulation. $\Delta\Psi\text{m}$ shift was profound by the 12 h after treatment and with greater accumulation of ROS over the same interval. Sequential interval study of cytochrome-c activity suggested that activity greatly increased by the 12 h and thereafter remained constant with no further significant change. This indicates that initiation of cytochrome-c dispersal into the cytoplasm, might be dependent on

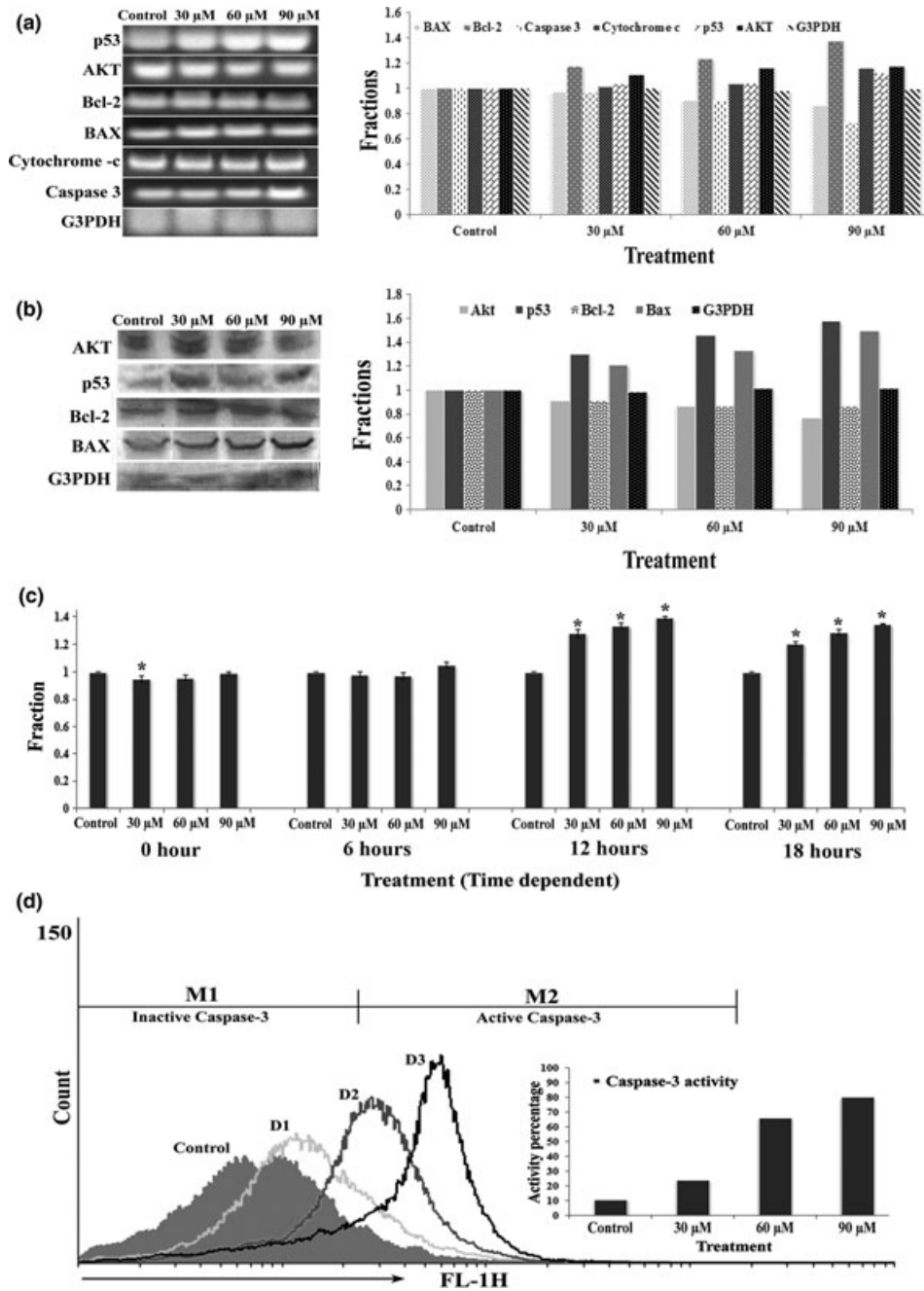


Figure 7. RT-PCR (a) and western blot analysis (b) of different mRNA and proteins revealed reduction in population growth inducers and anti-apoptotic genes/proteins. (c) Time-dependent cytochrome-c assay indicated that activity of cytochrome-c was upregulated at the 12 h interval. (d) caspase-3 assay determined this death protein's activity in response to quercetin treatment at concentrations of 30, 60 and 90 μ M, by flow cytometric analysis.

ROS generation with $\Delta\Psi_m$ disruption, and could thereby initiate apoptosis.

Cell cycle arrest and cell population growth inhibition may induce greater sensitivity of cells to having more tumour suppressor proteins such as p53. This was

revealed by our observation that p53 expression was up-regulated alongside cell cycle arrest and cell population growth inhibition. With arrest of cell population expansion, expression of Akt (22), an important cell differentiation and proliferative molecule, was down-regu-

lated. One hypothesis to explain this could be that there is p53-AKT crosstalk after quercetin induction. One earlier study (23) has documented that deactivated Akt cannot inhibit Bax translocation into mitochondria. Deactivated Akt induces Bax to do this by altering mitochondrial membrane polarization, eases passage of cytochrome-c being released. Cytochrome-c in the cytosol thus obtains sufficient space for activity to initiate activation of the caspase cascade. Through this cascade, caspase-3 becomes activated, and is responsible for inter-nucleosomal DNA fragmentation, a marked feature of apoptotic cell death.

Apoptosis is tightly regulated by anti-apoptotic and pro-apoptotic effector molecules, including proteins of the Bcl-2 family, and can be mediated by several different pathways. They are crucial protagonists in mitochondrial apoptosis (24). The alterations in the level of Bax and Bcl-2 are decisive features determining whether cells will undergo apoptosis, or would be directed to a survival pathway (25). Down-regulation of Bcl-2 and upregulation of Bax protein in the cytosol in quercetin-treated cells suggests the possible molecular mechanisms involved through which quercetin induces apoptosis in cells, here of cervical cancer.

It is already known that as levels of cytochrome-c increase in the cytosol, it interacts with Apaf-1 and ATP to form a complex with procaspase-9 (apoptosome), leading to activation of pro-caspase-9 and caspase-3; activated caspase-3 is the key executioner of apoptosis (26). We found that quercetin treatment of HeLa cells resulted in dose-dependent activation of caspase-3, sequentially initiating apoptosis as demonstrated by externalization of phosphatidylserine with DNA fragmentation initiation.

In conclusion, from results of the present study, we can deduce that quercetin has the potential to intercalate with cell DNA with a shift of 10 nm. This capacity may control regulatory action of quercetin on the cancer cells. Quercetin also has the ability to generate ROS-mediated depolarization of mitochondrial membrane potential, initiating release of cytochrome-c.

Acknowledgements

This work was partially supported by a grant sanctioned to Prof. A.R. Khuda-Bukhsh, Department of Zoology, University of Kalyani, by Boiron Laboratories, Lyon, France. We are also greatly thankful to Mr Chanchal Kumar Das and Prof. Prasanta Kumar Das of National Cultivation of Science, Kolkata for helping us in CD spectroscopic studies.

Conflict of interest

None to declare.

References

- 1 Neuhauser ML (2004) Dietary flavonoids and cancer risk: evidence from human population studies. *Nutr. Cancer* **50**, 1–7.
- 2 Häkkinen SH, Kärenlampi SO, Heinonen IM, Mykkänen HM, Törrönen AR (1999) Content of the flavonols quercetin, myricetin, and kaempferol in 25 edible berries. *J. Agric. Food Chem.* **47**, 2274–2279.
- 3 Nöthlings U, Murphy SP, Wilkens LR, Henderson BE, Kolonel LN (2007) Flavonols and pancreatic cancer risk: the multiethnic cohort study. *Am. J. Epidemiol.* **166**, 924–931.
- 4 Paliwal S, Sundaram J, Mitragotri S (2005) Induction of cancer-specific cytotoxicity towards human prostate and skin cells using quercetin and ultrasound. *Br. J. Cancer* **92**, 499–502.
- 5 Zhang W, Zhang F (2009) Effects of quercetin on proliferation, apoptosis, adhesion and migration, and invasion of HeLa cells. *Eur. J. Gynaecol. Oncol.* **30**, 60–64.
- 6 Huang LQ, Zhang W, Yang Y, Tao L (2009) Effects and its mechanism of quercetin on cervical cancer HeLa cells. *Zhonghua Fu Chan Ke Za Zhi.* **44**, 436–439.
- 7 Priyadarsini RV, Murugan RS, Maitreyi S, Ramalingam K, Karunakaran D, Nagini S (2010) The flavonoid quercetin induces cell cycle arrest and mitochondria-mediated apoptosis in human cervical cancer (HeLa) cells through p53 induction and NF- κ B inhibition. *Eur. J. Pharmacol.* **649**, 84–91.
- 8 Green JA (2001) Clinical trials in cancer. *Br. J. Cancer* **104**, 1521–1522.
- 9 Swenson DH, Li LH, Hurley LH, Rokem JS, Petzold GL, Dayton BD *et al.* (1982) Mechanism of Interaction of CC-1065 (NSC 298223) with DNA. *Cancer Res.* **42**, 2821–2828.
- 10 Palumbo M, Capasso L, Palù G, Marcianimagno G (1985) Conformational aspects of drug-DNA interactions: studies on anthracycline antibiotics and psoralen derivatives. *J. Biosci.* **8**, 689–697.
- 11 Gottlieb TM, Leal JML, Seger R, Tay Y, Oren M (2002) Crosstalk between Akt, p53 and Mdm2: possible implications for the regulation of apoptosis. *Oncogene* **21**, 1299–1303.
- 12 Bishayee K, Mukherjee A, Paul A, Khuda-Bukhsh AR (2012) Homeopathic mother tincture of Conium initiates reactive oxygen species mediated DNA damage and makes HeLa cells prone to apoptosis. *Int. J. Genuine Traditional Med.* **2**, e26. doi: 10.5667/tang.2012.0018.
- 13 Garbett NC, Patricia A, Ragazzon PA, Chaires JB (2007) Circular dichroism to determine binding mode and affinity of ligand–DNA interactions. *Nat. Protoc.* **2**, 3166–3172.
- 14 Liang CC, Park AY, Guan JL (2007) In vitro scratch assay: a convenient and inexpensive method for analysis of cell migration in vitro. *Nat. Protoc.* **2**, 329–333.
- 15 Paul A, Bishayee K, Ghosh S, Mukherjee A, Sikdar S, Chakraborty D *et al.* (2012) Chelidonine isolated from ethanolic extract of *Chelidonium majus* promotes apoptosis in HeLa cells through p38-p53 and PI3K/AKT signalling pathways. *Zhong Xi Yi Jie He Xue Bao.* **10**, 1025–1038.
- 16 Chakraborty D, Bishayee K, Ghosh S, Biswas R, Mandal SK, Khuda-Bukhsh AR (2012) [6]-gingerol induces caspase 3 dependent apoptosis and autophagy in cancer cells: Drug-DNA interaction and expression of certain signal genes in HeLa cells. *Eur. J. Pharmacol.* **694**, 20–29.

- 17 Chakraborty D, Mukherjee A, Sikdar S, Paul A, Ghosh S, Khuda-Bukhsh AR (2012) [6]-Gingerol isolated from ginger attenuates sodium arsenite induced oxidative stress and plays a corrective role in improving insulin signalling in mice. *Toxicol. Lett.* **210**, 34–43.
- 18 Mandal SK, Biswas R, Bhattacharyya SS, Paul S, Dutta S, Pathak S *et al.* (2010) Lycopodin from *Lycopodium clavatum* extract inhibits proliferation on HeLa cells through induction of apoptosis via caspase-3 activation. *Eur. J. Pharmacol.* **626**, 115–122.
- 19 Fulda S, Debatin KM (2006) Extrinsic versus intrinsic apoptosis pathways in anticancer chemotherapy. *Oncogene* **25**, 4798–4811.
- 20 Shahabuddin MS, Gopal M, Raghavan SC (2007) Intercalating cytotoxic, antitumour activity of 8-chloro and 4-morpholinopyrimido [4',5':4,5]thieno(2,3-b)quinoline. *J. Photochem. Photobiol. B* **3**, 139–146.
- 21 Atlantea A, Calissano P, Bobba A, Azzariti A, Marra E, Passarella S (2000) Cytochrome c is released from mitochondria in a reactive oxygen species (ROS)-dependent fashion and can operate as a ROS scavenger and as a respiratory substrate in cerebellar neurons undergoing excitotoxic death. *J. Biol. Chem.* **275**, 37159–37166.
- 22 Gottlieb TM, Leal JFM, Seger R, Taya Y, Oren M (2002) Cross-talk between Akt, p53 and Mdm2: possible implications for the regulation of apoptosis. *Oncogene* **21**, 1299–1303.
- 23 Tsuruta F, Masuyama N, Gotoh Y (2002) The phosphatidylinositol 3-kinase (PI3K)-Akt pathway suppress Bax translocation to mitochondria. *J. Biol. Chem.* **277**, 14040–14047.
- 24 Vento MT, Zazzu VZ, Loffreda A, Cross JR, Downward J, Stoppelli MP *et al.* (2010) Prf2 is a novel Bcl-xL/Bcl-2 interacting protein with the ability to modulate survival of cancer cells. *PLoS One* **5**, 1–13.
- 25 Tsujimoto Y, Shimizu S (2000) Bcl-2 family: life-or-death switch. *FEBS Lett.* **466**, 6–10.
- 26 Mantena SK, Sharma SD, Katiyar SK (2006) Berberine, a natural product, induces G1-phase cell cycle arrest and caspase-3-dependent apoptosis in human prostate carcinoma cells. *Mol. Cancer Ther.* **5**, 296–308.